Postprint of: Tiwari N. K., Jha A. K., Singh S. P., Akhtar M. J., Estimation of Broadband Complex Permeability Using SIW Cavity-Based Multimodal Approach, in IEEE Transactions on Instrumentation and Measurement, vol. 69, no. 9 (2020), pp. 6571-6581,
DOI: 10.1109/TIM.2020.2969590

Estimation of Broadband Complex Permeability using SIW Cavity based Multimodal Approach

Nilesh K Tiwari, *Student Member, IEEE,* Abhishek K Jha, *Member, IEEE,* S. P. Singh, *Student Member, IEEE,* M Jaleel Akhtar, *Senior Member, IEEE*

***Abstract*— In this paper, an attractive multimodal substrate integrated waveguide (SIW) based methodology is presented for the characterization of magnetic materials in the broadband microwave frequency. The proposed approach alleviates the need for multiple SIW cavity design for broadband characterization of magnetic samples. It employs the modified technique to consider the effect of finite sample size, sinusoidal field variation, operating mode numbers, and substantial perturbation, which were not considered before for magnetic testing using the conventional SIW cavity. Effect of the relatively smaller quality factor and higher frequency shift, which were the two prime limiting factors with the conventional SIW cavity, are relaxed here. A unified closed-form expression is developed from the first principle to retrieve the complex permeability. The proposed technique is numerically verified using the full-wave electromagnetic (EM) simulator for several dispersive and non-dispersive standard samples; thereafter, it is validated for the estimation of complex permeability of synthesized dispersive magnetic composites. It is found that the developed approach can characterize the dispersive magnetic composites, where the permeability value varies from paramagnetic to diamagnetic range, with improved accuracy than that of the conventional cavity perturbation approach. The modified formulation provides 34% and 12% better estimation of loss tangent and real permeability, respectively, as compared with the conventional technique. The uncertainty analysis for sample volume, sample misalignment, and the possible air gap is also carried out in detail. The proposed scheme typically provides more than 92% and 84% accuracy in the measured values of real permeability and loss tangent data, respectively, for various synthesized magnetic samples in broadband of microwave frequency (10 GHz - 22 GHz).**

***Index Terms*— Broadband multimodal technique, complex permeability, multimode, magnetic materials, substrate integrated cavity.**

I. Introduction

THE microwave material characterization using the cavity perturbation approach was started in the early sixties [1]-[3]. The material perturbation approach (MPA), developed from Maxwell's equations, has quite involved mathematical expressions related to the physical parameters of the cavity and the constitutive electromagnetic parameter of the test specimen. Later, employing certain approximations in the material perturbation approach, the closed-form analytical expressions of the material constitutive parameters were developed in terms of the resonant frequency and quality factor of the metallic cavity [1]-[7]. The major assumptions that are made to develop the approximately closed formulation of MPA are as follows: the high ratio of the cavity to sample volume, minimal sample size, unsubstantial perturbation, and high-quality factor. These assumptions still help in the calculation of complex permittivity of the test specimen; however, with limited accuracy [4]-[6]. A number of researchers have contributed to improving the accuracy of MPA using various modified techniques [5]-[8]. Recently, the sinusoidal field variation and resonant mode number of the cavity are included to improve the accuracy of MPA [8]. In short, the estimation of complex permittivity using the conventional metallic cavity is being gone through a series of modifications, which helps in finding both the real and imaginary parts of the complex permittivity with reasonable accuracy [4]-[8]. Similarly, the extraction of complex permeability of test specimens involving MPA is being modified to improve accuracy [9]-[14]. Recently, it is reported that the complex permeability of test specimen placed inside a metallic cavity can be retrieved with more than 40% accuracy as compared with the conventional MPA [13]. Later, a generalized method for waveguide cavity is proposed, which relaxes several approximations related to MPA, for the magnetic characterization of arbitrary length samples usually used in the microwave material industry [15].

Despite the excellent accuracy of MPA applied to the waveguide cavity, the direct application of this technology is quite limited due to the lack of easy integration of the metallic cavity with the planar microwave circuits. It is, therefore, in recent years, microwave research is highly directed to develop compact planar devices and material characterization systems to comply with state of the art planar integrated circuit technology (PICT) [16]-[19]. Unlike the bulky and costly metallic waveguide technology, the substrate integrated waveguide (SIW) technology is compatible to PICT, and easier to realize the planar and compact cavity structures [20]-[23]. However, the closed-form approximation developed for MPA using the metallic cavity becomes quite tricky for SIW cavity, which is discussed in [24]. In [24], MPA is modified for extracting the complex permittivity of dielectric test specimen placed inside the SIW cavity. However, the formulation of complex permeability of magnetic test specimens using a modified SIW cavity is currently not available in literature [25]. The SIW cavity-based MPA for retrieval of complex permeability as reported in [25] is mainly

based on the conventional perturbation approach. This approach mainly requires the use of standard magnetic samples with their known value of complex permeability at the required frequency, which happens to be quite impractical and uneasy for designing a microwave device operating at wideband of frequency. Another drawback of the SIW cavity-based magnetic characterization scheme is the single frequency measurement, which means that multiple frequency measurement using this scheme needs several SIW resonators tuned to resonate at desired frequency points. Also, the designed SIW cavity operates quite close to its dominant mode thus restricting the size, quality factor, volume ratio, and high frequency operating capability. Therefore, it is required to develop a unified MPA using SIW cavity, which can be easily used for the characterization of magnetic materials at wideband of microwave frequency. To the best of author's knowledge, this kind of approach is currently not available in the literature.

The proposed technique presents the broadband complex permeability characterization of magnetic composites by developing the unified closed formulation for multi-mode operation, which is the first of its kind using SIW cavity. The proposed formulation mainly relaxes the dominant mode operation requirement by suitably using the under-coupled SIW cavity and then considering the operating mode number in the formulation. Here it is to be noted that the proposed SIW structure is designed using the modified feed topology to facilities the under-coupled higher-order mode operation, which helps to improve the quality factor. Moreover, the proposed formulation considers the sinusoidal variation of the magnetic field over the sample cross-section to relax the constant field approximation and infinitesimally small sample size. Another primary assumption that the resonant frequency before and after perturbation must be equal and *Q*-factor should be quite high is also relaxed by adequately modifying the conventional formulation. Firstly, the proposed scheme is numerically verified by performing a wideband complex permeability estimation of the magnetic test specimens. These test specimens have dispersive magnetic properties, which are defined by the first order Debye model at various TE_{10p} modes. After that, various arbitrary magnetic samples are tested, and their results are quantified, where the error estimated using the proposed method is compared with the conventional technique. Finally, four dispersive magnetic composites are synthesized, which are then tested using the proposed technique, while placing them sequentially inside the fabricated SIW cavity. The measured results obtained in the wideband microwave frequency are presented in terms of the accuracy of the proposed technique for both the paramagnetic and diamagnetic samples under test.

II. Numerical Design and Analytical Formulation

A. Modified SIW cavity model

A numerical simulation model of the proposed SIW cavity-based planar structure, which is used for the complex permeability extraction of the test specimen is given in Fig1. The modified SIW cavity possesses the wideband impedance matching by incorporating a transformation of the input impedance of quasi TEM of microstrip line to TE_{10p} mode of SIW cavity through the TE_{10} mode of SIW waveguide unlikely the conventional quasi TEM to TE_{10p} conversion [24]. It basically helps the SIW cavity to operate in under-coupled state over all the specified modes with significantly higher *Q*-factor than that of conventional over-coupled dominant mode operated SIW cavity. The full-wave electromagnetic solver, the CST-MWS, is employed to perform the numerical analysis of the proposed approach. The design parameters of the cavity are a = 14 mm, d = 1 mm, l = 63 mm, $w = a-2d$, w_1 = 6 mm, w_2 =3 mm, and s = 1.5 mm, while the sample dimensions are a_1 = 10 mm, b = 0.8 mm, and l_1 = 1 mm. From this figure, it can be seen that unlike the case of complex permittivity measurement [13], the test specimen is placed horizontally along the width of the SIW cavity.

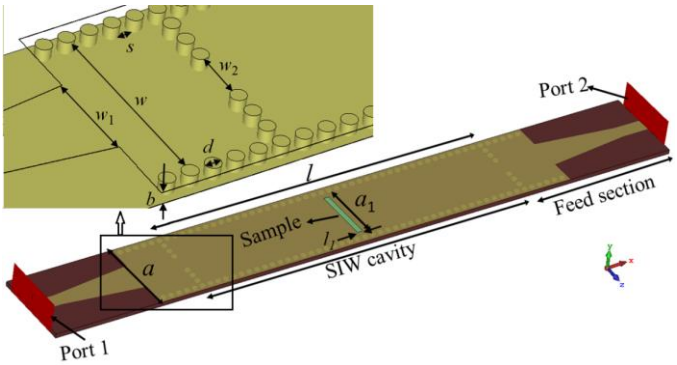

Fig.1. Proposed SIW cavity designed on the substrate with various dimensions and sample position used in numerical simulation. A detailed layout of the coupling section is shown in the inset with a transparent Roger RT-5880 substrate (ε_r =2.2-*j*0.002, μ_r = 1), and the upper layer of metallization.

Since the planar SIW uses the via to mimic the perfect boundary condition (PEC), the expression of the electromagnetic field of the SIW cavity can be given in terms of the effective width and the effective length as follows:

$$\begin{aligned} E_y &= E_{y0}\sin(k_x x)\sin(k_z z) \\ H_z &= \frac{2w_{eff}}{\lambda_g}\frac{\pi}{j\omega\mu_0\mu_s w_{eff}}\cos(k_x x)\sin(k_z z)E_{y0} \\ H_x &= \frac{j\pi}{\omega\mu_0\mu_s w_{eff}}\sin(k_x x)\cos(k_z z)E_{y0} \end{aligned} \quad (1)$$

where $w_{eff} = (a-d) - 1.08\frac{d^2}{s} + 0.1\frac{d^2}{(a-d)}$

$$l_{eff} = (l-d) - 1.08\frac{d^2}{s} + 0.1\frac{d^2}{(l-d)}$$

$$k_z = \pi / w_{eff},\ k_x = p\pi / l_{eff},\ p = 2,\ 4,\ 6,\ 8\ldots$$

where E_{y0} λ_g and μ_s denote the maximum value of the electric field, guided wavelength inside the SIW cavity, and complex permeability of the SIW substrate, respectively [3], [26]. From (1), it can be observed that the placement of test specimens as shown in Fig 1, mostly perturbs the *z*- component of the magnetic field of SIW cavity operating in TE_{10p} mode with p =

even number, while the electric field of cavity remains unperturbed. The contour plots of the electric field and the magnetic field of the TE_{10p} mode (p = 4) of SIW cavity, where sample location is also identified, are provided in Fig. 2 that clarifies our proposition. From Figs. 2(a) and 2(c), it can be observed that the electric field and the x-component of the magnetic field patterns are absent at the center of SIW cavity around the sample position; therefore, E_y and H_x of (1) are considered to be unperturbed. However, z-component of the magnetic field, H_z has maximum intensity at the center of the cavity around the sample under test; therefore, perturbation of H_z is considered in developing the modified MPA.

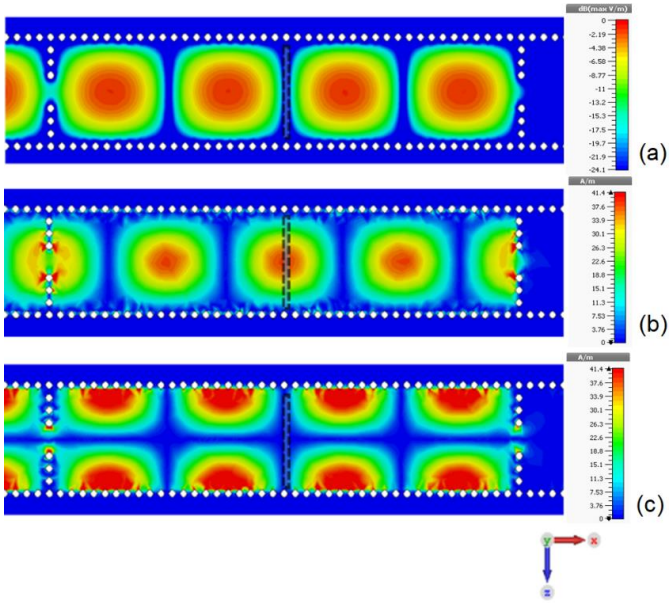

Fig.2. Plot of absolute (a) electric field, (b) z-component and (c) x-component of the magnetic field for TE_{10p} mode of SIW cavity (without sample) corresponding to p = 4, where dotted black lines denotes sample position.

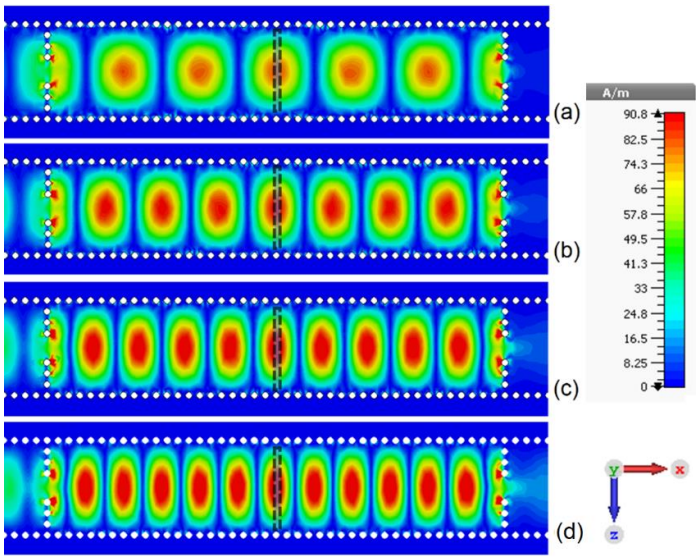

Fig. 3. Plot of absolute value of H_z for TE_{10p} mode corresponding to (a) p = 6, (b) p = 8, (c) p = 10, and (d) p = 12, where the position of sample is shown with dotted black lines at the center of the SIW cavity without sample loading.

Before using this generalized concept of selective perturbation for all the even modes of TE_{10p} mode, the absolute value of H_z is plotted for p = 6, 8, 10, and 12 in Fig.3. From this figure, it can be observed that the H_z component shows sinusoidal variation over the sample length for all the even modes. The consideration of this selective perturbation will be taken care of in the next section for the retrieval of complex permeability of the test samples.

B. The Mathematical formulation of complex permeability

The complex permeability of the test specimen placed horizontally at the center of the SIW cavity structure can be related to the two measurable physical quantities viz. the resonant frequency and the quality factor of the cavity using the perturbation approach. A standard material perturbation relation corresponding to the test specimen with complex permeability $\mu_{rT} = \mu'_{rT} - j\mu''_{rT}$ loaded on the SIW cavity with substrate material having complex permeability $\mu_{rS} = \mu'_{rS} - j\mu''_{rS}$ can be written by modifying the standard relation of MPA for metallic cavity [12], 13]

$$\frac{\Delta f}{f_T} = \frac{f_T - f_0}{f_T} = -\frac{\iiint_{V_T}\left(\frac{\mu_{rT}}{2\mu_{rS}} - \frac{1}{2}\right)\vec{H}_0^* \cdot \vec{H}_T dv}{\iiint_{V_C}\left|\vec{H}_0\right|^2 dv} \tag{2}$$

where $f_T = f_{Tr} + jf_{Ti}$ and $f_0 = f_{r0} + jf_{i0}$ represent the complex resonant frequency corresponding to the perturbed and the unperturbed conditions. The symbols H_T and H_0 are the magnetic field component of the SIW cavity corresponding to the perturbed and the unperturbed conditions; V_C and V_T are the volumes of the cavity and the test specimen [12], [24]. As explained and discussed in the preceding section, the introduction of a magnetic sample at the center of the SIW cavity (as shown in Fig. 1) only perturbs z-component of the magnetic field, as shown in Figs. 2 and 3. Therefore, the expression (2) can be further simplified, especially for the infinitesimally small bar-shaped test specimen assuming the small perturbation, high Q, and constant magnetic field intensity over the test specimen [13]. Using these assumptions, the conventional closed formulations of real and imaginary parts of the complex permeability can be given as:

$$\mu'_{rC} = \left(\frac{(f_{0r} - f_{Te})V_C\left(l_{eff}^{\ 2} + w_{eff}^{\ 2}p^2\right)}{2f_{Tr}w_{eff}^{\ 2}p^2V_S} + 1\right)\mu'_{rS}$$
$$\mu''_{rC} = \mu'_{rS}\left(\frac{V_C\left(l_{eff}^{\ 2} + w_{eff}^{\ 2}p^2\right)}{4w_{eff}^{\ 2}p^2V_S}\right)\left(\frac{1}{Q_T} - \frac{1}{Q_0}\right) + \mu'_{rC}\tan\delta_S \tag{3}$$

The formulation (3) contains several approximations such as infinitesimally small test specimens with constant magnetic field intensity over the sample under test, small frequency shift (f_T = f_0), and very high Q ([1/Q] ~ 10^{-4}). These approximations work well only for the simplification of the approach at the expense of accuracy in the retrieval of complex permeability, which has been recently reported considering the metallic waveguide cavity [13]-[14]. However, the SIW cavity has many advantages over its

counterpart, i.e., metallic waveguide cavity such as low cost, low weight, easy integration with monolithic microwave integrated circuit (MMIC). It is, therefore, quite necessary to modify the standard cavity perturbation applicable for SIW cavity dealing with magnetic samples, which is currently missing in the literature. Moreover, the higher-order modes of TE_{10p} may not be considered for the conventional over-coupled SIW cavity, which limits the broadband retrieval of complex permeability using the multimodal technique.The exemption of higher-order modes in the broadband characterization of microwave material may necessitate the design of multiple SIW cavities operating at the lower or dominant mode [25]. However, at a higher frequency, the size of the SIW cavity corresponding to the dominant mode becomes quite small, and hence sample to cavity volume ratio gets further reduced, thus limiting the accuracy of conventional perturbation formulation. In our proposed approach, the effort has been made to utilize the higher operating modes of SIW cavity thus facilitating the high-frequency magnetic characterization while considering the design parameters corresponding to lower frequency region. For example, the TE_{10p} mode with p = 4, 6, 8, 10 and 12 are considered for multimodal characterization of test samples with the modified under-coupled SIW cavity using the proposed technique. The modified formulation of MPA can be derived by relaxing some of the significant assumptions of the conventional technique e.g., an infinitesimally small sample placed in constant magnetic field is relaxed by considering the finite sample placed inside the actual magnetic field of the specified operating mode (4). Another major assumption that the quality factor is significantly large enough to neglect the Q^{-1} term, usually valid for a metallic cavity, is relaxed for the SIW cavity. The proposed formulation uses the actual unloaded Q factor of the SIW cavity in the absence of sample loading and external coupling [26]. The generalized perturbation relation given in (2) is now reconsidered while relaxing the major assumptions primarily neglected in the conventional approach. The values of sinusoidal magnetic field components can now be used in (2) to recalculate the shift in resonant frequency over the finite sample dimension $l_1 \times b \times a_1$, which can be written as (4). The finite integration used in the right-hand side of (4) can be solved with employing the trigonometric identities for getting the closed-form relation, which can be given as (5). The left-hand side of (5) is reformulated by relaxing some of the significant limitations such as negligibly small frequency shift (f_T=f_0), and very high Q [$(1/Q) \sim 10^{-4}$], which was employed earlier in our work [13], can be used to get the simplified expression as given in (6). The modified formulations (5)-(6) now consider the finite shift in resonant frequency andthe relatively smaller Q-factor associated with the SIW cavity by relaxing the assumptions *viz*. f_T=f_0 and negligence of Q^{-1}, respectively.

$$\frac{f_T - f_0}{f_T} = -\frac{4\pi^2 w_{eff}^{\ 2}\left(\omega\mu_0\mu_s w_{eff}\lambda_g\right)^{-2}\int_{(w_{eff}-a_1)/2}^{(w_{eff}+a_1)/2}\int_0^b\int_{(l_{eff}-l_1)/2}^{(l_{eff}+l_1)/2}\left(\frac{\mu_{rT}}{2\mu_{rS}}-\frac{1}{2}\right)N_1N_2\,dzdydx}{\int_0^{w_{eff}}\int_0^b\int_0^{l_{eff}}\left(D_1+D_2\right)dzdydx} \tag{4}$$

where, $N_1 = \left(0.5+0.5\cos\left(2k_x x\right)\right)$,

$N_2 = \left(0.5-0.5\cos\left(2k_z z\right)\right)$

$D_1 = 4\pi^2 w_{eff}^{\ 2} / \left(\omega\mu_0\mu_s w_{eff}\lambda_g\right)^2 \left(0.5+0.5\cos\left(2k_x x\right)\right)\left(0.5-0.5\cos\left(2k_z z\right)\right)$,

$D_2 = \left(\frac{\pi}{\omega\mu_0\mu_s w_{eff}}\right)^2 \left(0.5+0.5\cos\left(2k_z z\right)\right)\left(0.5-0.5\cos\left(2k_x x\right)\right)$

$$\frac{f_T - f_0}{f_T} = -\left(\frac{\mu_{rT}}{2\mu_{rS}}-\frac{1}{2}\right)4w_{eff}^{\ 2}\left(1-\frac{\sin k_z a_1}{k_z a_1}\cos\left(k_z w_{eff}\right)\right)\left(4w_{eff}^{\ 2}+\lambda_g^{\ 2}\right)^{-1}\left(1+\frac{\sin k_x l_1}{k_x l_1}\cos\left(k_x l_{eff}\right)\right)\frac{V_S}{V_C} \tag{5}$$

$$\frac{\Delta f}{f_T}=\frac{f_T-f_0}{f_T}=\frac{\left(f_{Tr}-f_{0r}\right)+j\left(f_{Ti}-f_{0i}\right)}{f_{Tr}\left(1+j\,\frac{f_{Ti}}{f_{Tr}}\right)}\equiv -x+jy\Bigg|_{f_T=f_{Tr}+jf_{Ti},\,F=\frac{f_{Tr}}{2f_{Ti}},F_0=\frac{f_{0r}}{2f_{0i}}} \tag{6}$$

$$\text{where, } x=\frac{\left(f_{0r}-f_{Tr}\right)+F\left(F_0 f_{0r}-Ff_{Tr}\right)}{f_{Tr}\left(1+F^2\right)}, y=\frac{f_{0r}\left(F-F_0\right)}{f_{Tr}\left(1+F^2\right)}, F=\frac{\left(1-\left|S_{21T}\right|\right)}{2Q_T}, F_0=\frac{\left(1-\left|S_{210}\right|\right)}{2Q_0}$$

$$\mu'_{rP}=\left(\frac{2xV_C\left(l_{eff}{}^2+w_{eff}{}^2p^2\right)}{w_{eff}{}^2p^2V_S\left(1-\frac{\sin k_z a_1}{k_z a_1}\cos\left(k_z w_{eff}\right)\right)\left(1+\frac{\sin k_x l_1}{k_x l_1}\cos\left(k_x l_{eff}\right)\right)}+1\right)\mu'_{rS}$$

$$\mu''_{rP}=\mu'_{rS}\left(\frac{2yV_C\left(l_{eff}{}^2+w_{eff}{}^2p^2\right)}{w_{eff}{}^2p^2V_S\left(1-\frac{\sin k_z a_1}{k_z a_1}\cos\left(k_z w_{eff}\right)\right)\left(1+\frac{\sin k_x l_1}{k_x l_1}\cos\left(k_x l_{eff}\right)\right)}\right)+\mu'_{rP}\tan\delta_S \tag{7}$$

$$\tan\delta_P=\mu''_{rP}\mu'^{-1}_{rP}$$

From (5) and (6), one can quickly notice that these relations are now able to consider various constraints associated with the SIW cavity, which were primarily neglected in the literature. More specifically, the modified under-coupled SIW cavity in conjunction with the modified formulations (5)-(7) provides the more realistic approach to calculate multimodal permeability for finite sample size with considering actual sinusoidal field variation by relaxing the conventional approximations i.e., constant magnetic field over infinitesimally small sample region, negligible perturbation ($f_T = f_0$), and very high Q [$(1/Q) \sim 10^{-4}$]. Thus, for broadband estimation of complex permeability, the proposed modified multimodal cavity and associated formulations may provide a better alternative than designing multiple single-mode cavities operating at lower frequency [25]. Comparing the real and imaginary terms of the right-hand side of (5) and (6), the expression of complex permeability can be given as (7). Using the set of relationships given in (7), the complex permeability of magnetic test specimens can be reformulated in the broad range of operating frequency by considering the multi-mode approach. Moreover, the proposed formulation is explicitly derived in terms of known or measurable parameters; hence, the requirement of the standard magnetic sample as the reference can be alleviated [25]. It is worth to mention here that alleviation of the standard/reference sample in the proposed method is quite advantageous as compared with the standard method, which can be easily explained by comparing (3) and (7). As discussed earlier, formulations (3) are a result of a number of approximations; therefore, the measurement of reference samples could be useful to normalize the parameters in terms of two measurable parameters, i.e. resonant frequency and quality factor [25]. This normalization somehow improves the accuracy of the standard method by computing the various constants involved in the formulation [25]. However, the accuracy of the standard scheme becomes entirely dependent on the values of complex permeability of the reference test specimen at the required frequency. This basically means that an error in standard value of the magnetic constants of the reference magnetic sample can multiply the error in the extracted magnetic parameter. However, the proposed under-coupled SIW cavity-based approach follows the direct estimation of complex permeability with the help of modified analytical formulation as given in (7), which relaxes the most of the earlier assumptions of MPA used in developing (3). The retrieval of complex permeability independent from the reference sample is quite advantageous as compared with the calibration based approach [25].

III. Estimation of Complex Permeability and Validation of Proposed Technique

A. Calculation of Complex Permeability Using Numerical method

In this section, the closed-form relationship developed in the preceding section is used to calculate the complex permeability of test specimens in the broad frequency range using the numerically generated scattering coefficient for different values of complex permeability. The numerical 2-port SIW model for generating the scattering parameters is shown in Fig. 1. The proposed scheme is tested for its suitability at broadband microwave frequency, the complex permeability of the magnetic sample under test is considered to be varying according to the Debye model. A first-order approximation of the Debye model with the values of relative permeability at the low-frequency limit, μ_0, relative permeability at the high-frequency limit μ_∞, and the

characteristic relaxation time of the medium τ are chosen to be 2, 1 and $6\text{x}10^{-12}$ s. The Debye model provides the values of relative permeability and magnetic loss factor varying in the range of 1.88 to 1.59 and 0.33 to 0.49, respectively, for the frequency range 10 GHz – 22 GHz, which seems to be a good approximation under the Snoek's limit [27].

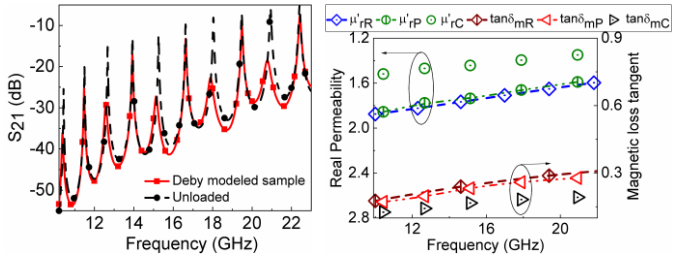

(a) (b)

Fig. 4. The plot of (a) transmission curves for various operating TE_{10p} modes related with p = 4 to 13, and (b) actual values of complex permeability calculated from Debye model and the estimated values of complex permeability using our proposed scheme.

The finite-difference-time-domain method (FDTD) method is used to calculate the 2-port scattering parameters. The values of S_{21} evaluated for various TE_{10p} modes of the cavity related with p = 4, 5, 6, 7 …13 are plotted in Fig. 4(a), which are found to be operating in the ultra-wide microwave frequency range from 10-23 GHz. From Fig. 4(a), it may be noted here that the introduction of Debye model of the magnetic sample selectively perturbs the TE_{10p} modes with p = even number, while the resonant frequency peaks corresponding to p = odd number are unchanged, which is also verified according to the modal analysis in the preceding section. Therefore, the information of resonant frequency and quality factor for both the unloaded and loaded cases related to p = 4, 6, 8, 10, and 12 are used to calculate the complex permeability using the newly developed formula (7) and plotted in Fig. 4(b). From Fig. 4(b), it can be observed that the values of relative permeability μ'_{rC} and magnetic loss tangent $\tan\delta_{mC}$ calculated with the conventional formula (3) are not in the excellent agreement with the reference (actual) values of relative permeability μ'_{rR} and magnetic loss tangent $\tan\delta_{mR}$, which were provided to the magnetic specimen using the first order Debye approximation. On the contrary, the relative permeability μ'_{rP} and magnetic loss tangent $\tan\delta_{mP}$ calculated using the proposed formulation (7) are found to be in substantial agreement with the values of μ'_{rR} and $\tan\delta_{mR}$, which closely follows the dispersive nature of the actual data as well.

After testing the proposed scheme with the dispersive sample as defined by the Debye model, the technique is applied to a number of standard non-dispersive samples having various complex permeability values. Therefore, in the next step, various magnetic test specimens with arbitrary values of the complex permeability, which includes low-loss and moderate-loss samples, are considered viz. A (1.2-j0.048), B (1.4-j0.084), C (1.6-j0.16), D (1.5-j0.075), E (1.7-j0.136), and F (1.3-j0.195), where the sample size is considered as 10 mm x 0.8 mm x 1 mm. The numerically generated S_{21} data corresponding to even modes (i.e., p = 4, 6, 8, 10, and 12) are shown in Fig. 5, where the unloaded condition is explicitly presented by '0'.

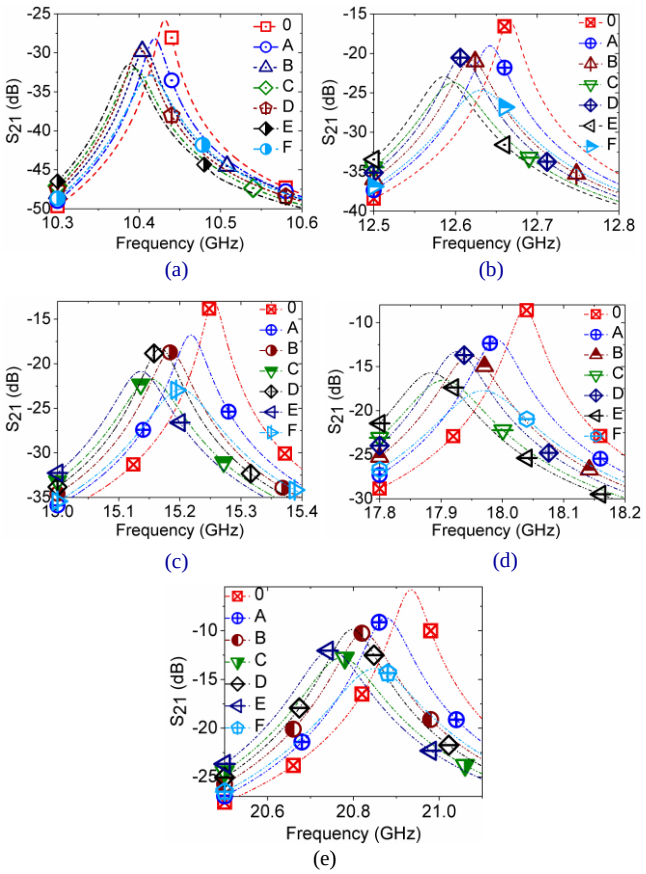

Fig. 5. Plot of unloaded and loaded transmission curves for various standard test specimen (A, B, C, D, E and F) associated with TE_{10p} where (a) p = 4, (b) p = 6, (c) p =8, (d) p = 10, (e) p = 12.

From Figs. 5 (a)-(e), it is observed that the resonant frequency and quality factor of the SIW cavity get significantly changed while following the change in complex permeability of the test specimen. For example, close observation of Fig. 5 suggests that an increase in the real part of the complex permeability and magnetic loss tangent of test specimen results in a decrease in the resonant frequency and an increase in the insertion loss, respectively. The resonant frequency and quality factor for each case are noted and processed using the developed formula (7) for estimation of the complex permeability. For a fair comparison, the complex permeability of each standard magnetic sample is also calculated using the conventional perturbation formula (3) that provides a relative error analysis with (7). The obtained results are arranged sequentially as the real and the imaginary parts of the complex permeability and plotted in Fig. 6. Moreover, Fig.6 also contains the results of one diamagnetic sample G (0.9-j0.027) to show the applicability of proposed approach for diamagnetic to paramagnetic samples. In this figure, the estimated values of real and imaginary parts of the complex permeability calculated using (3) and (7) are plotted with

respect to the actual values, while the relative error is calculated for each sample under test and separately plotted for each TE_{10p} mode in the following figures. The relative error in real and loss tangent data is calculated as:

$$\begin{aligned} \exists \mu'_{ri} &= \left|\left(\mu'_{ri} - \mu'_{rs}\right) - \left(\mu'_{rA} - \mu'_{rs}\right)\right| \\ \exists \tan\delta_{mi} &= \left|\left(\tan\delta_{mi} - \tan\delta_{ms}\right) - \left(\tan\delta_{mA} - \tan\delta_{ms}\right)\right|_p, \\ i &= P, C, \text{and } p = 4,6,8,10,12. \end{aligned} \tag{8}$$

The symbols in (8) have their usual meaning with subscripts *A*, *C*, *P*, and *S* representing the actual or original value, the value calculated using the conventional technique, the value calculated using the proposed technique, and the value related to the substrate of SIW cavity.

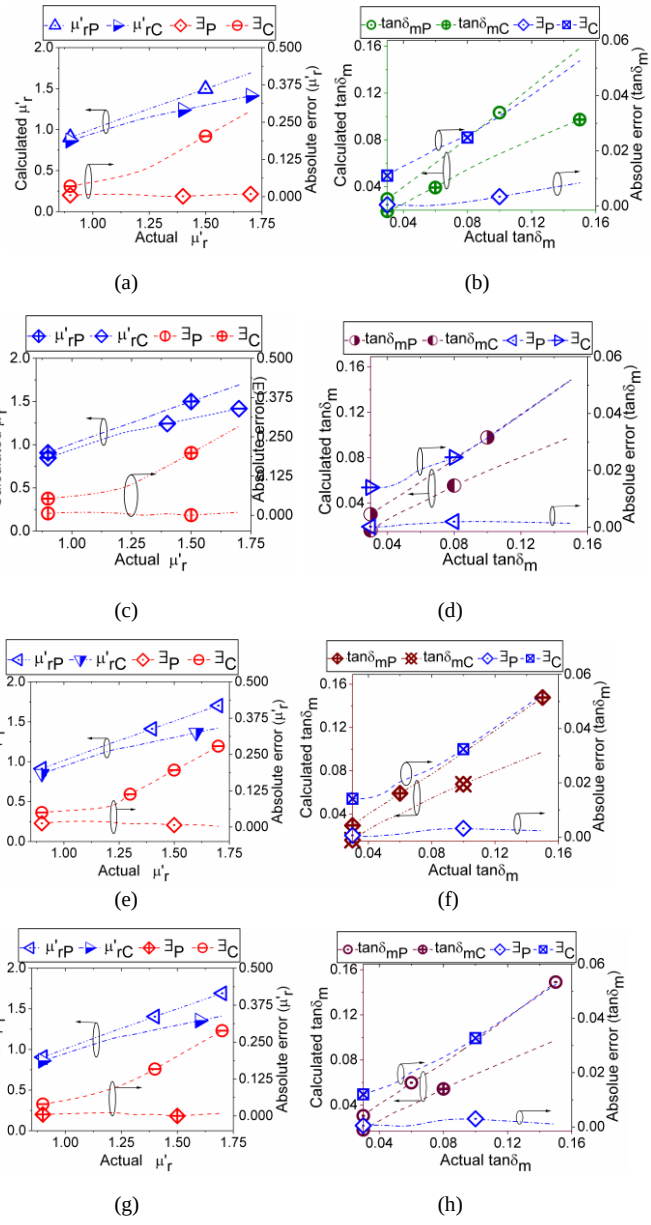

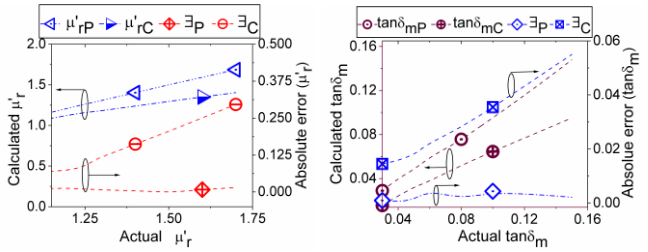

Fig. 6. Plot of real part of the complex permeability (a), (c), (e), (g), (i) and plot of loss tangent of the complex permeability (b), (d), (f), (h), (j) with relative error presented as absolute value where suffixes P and C represent results obtained using proposed and conventional technique, respectively. The real permeability and the loss tangent data of standard magnetic samples A, B, C, D, E and F associated with TE_{10p} mode for (a) and (b) p = 4, (c) and (d) p = 6, (e) and (f) p = 8, (g) and (h) p = 10, (i) and (j) p = 12, respectively. The actual values of magnetic sample are given at x-axis, they are A (1.2-*j*0.048), B (1.4-*j*0.084), C (1.6-*j*0.16), D (1.5-*j*0.075), E (1.7-*j*0.136), and F (1.3-*j*0.195), G (0.9-*j*0.027).

From Fig. 6, it can be ascertained that the proposed modified formulation can be used to calculate the complex permeability of low-loss and medium-loss magnetic samples quite accurately as compared with the conventional technique. It is mainly because the developed scheme considers several aspects of SIW cavity limitation viz. the finite volume of sample, sinusoidal magnetic field intensity, and the operating mode number; the proposed approach is much better than the conventional approach. From the error analysis, as given in Fig. 6, it is quite clear that the results obtained using proposed formula (7) are always better than the results obtained using conventional formula (3) in a wideband of microwave frequency, which is verified and found suitable for the characterization of a range of magnetic sample having arbitrary values of the complex permeability. In the next section, several synthesized magnetic samples, which are quite dispersive, and show the paramagnetic as well as diamagnetic behavior in the wideband of microwave frequency, are tested using the proposed scheme.

B. Retrieval of Complex Permeability of synthesized Magnetic Composites

After numerical verification of the proposed approach, the synthesized magnetic composites are tested using the developed formula. In this section, four different types of magnetic samples with various compositions of their constituent are considered in such a way that the dispersive nature of complex permeability can be easily observed in the ultra-wideband of microwave frequency. The synthesized magnetic materials under test are a barium hexaferrite sample, a Tb-doped ferrite (with Fe-nanoparticles) sample, and two samples of carbonyl iron/silicon rubber (CI/Si) composites with their weight by weight ratio 35/65, and 45/55. The composition of individual constituents and their weight proportion affects the overall value of the complex permeability. The synthesized magnetic samples for measurement using the developed approach are quite dispersive, which makes them paramagnetic (magnetic susceptibility greater than 0) to diamagnetic (magnetic susceptibility less than or equal to 0) in the wideband

microwave frequency. For a fair comparison, the reference values of the synthesized magnetic composites obtained using the standard cavity approach in addition to the dispersion model approach [14], [27]-[30] are also provided. A detailed measurement setup of the proposed approach is shown in Fig. 7. The PNA-L network analyzer (N5230C) from Agilent Technologies is used here to measure the S-parameter of the fabricated SIW cavity, which is connected through the set of coaxial cables and SMA connectors (Fig. 7). An appropriate IF bandwidth (70 Hz) and a number of frequency points (3201) are chosen accordingly to ensure better repeatability and measurement accuracy. Moreover, a full two-port Short-Open-Load-Thru (SOLT) calibration of the network analyzer is carried out before testing any test samples to remove the effect of a systematic error. The SIW is fabricated on 0.8 mm thick Roger RT-5880 substrate (ε_r=2.2-j0.002) with 35 µm thick metallization coating. The dimensions of the cavity sensor are kept the same as provided earlier as design parameters. The measured broadband transmission coefficient of the unloaded state is compared with the simulation data and shown in Fig.8, where a close match can be observed. The measured unloaded resonant frequencies corresponding to p = 4, 6, 8, 10, and 12 are found to be 10.431 GHz, 12.666 GHz, 15.254 GHz, 18.035 GHz, and 20.934 GHz, respectively.

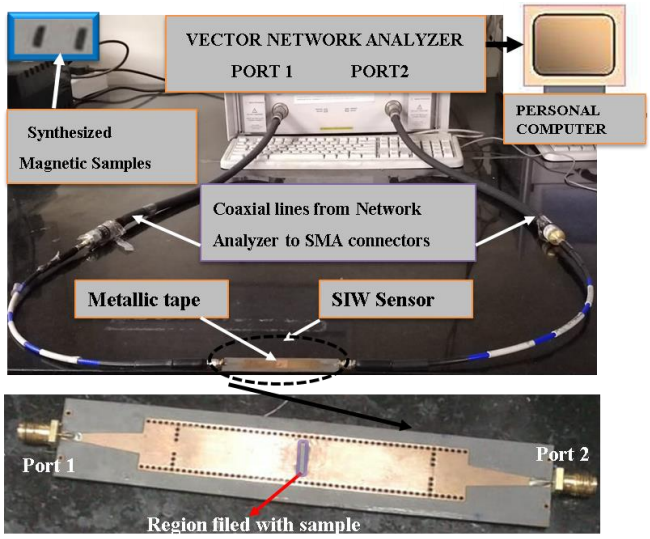

Fig.7. A typical experimental setup to estimate the complex permeability using the proposed SIW cavity-based technique.

The synthesized samples of dimensions 10 mm x 1 mm x 0.8 mm are sequentially placed in the sample region (Fig. 7), and the slot opening is closed with the help of 0.08 mm thick Cu-tape. The scattering parameters corresponding to each of the samples are then recorded to find the value of resonant frequency and quality factor with the help of vector network analyzer (VNA). The plot in Fig. 9 shows the obtained scattering parameters related to each of the four synthesized magnetic composites when tested around the TE_{10p} resonating modes for p = 4, 6, 8, 10, and 12.

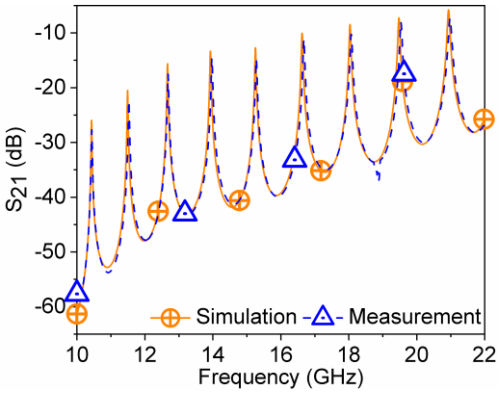

Fig.8. Broadband unloaded transmission coefficients

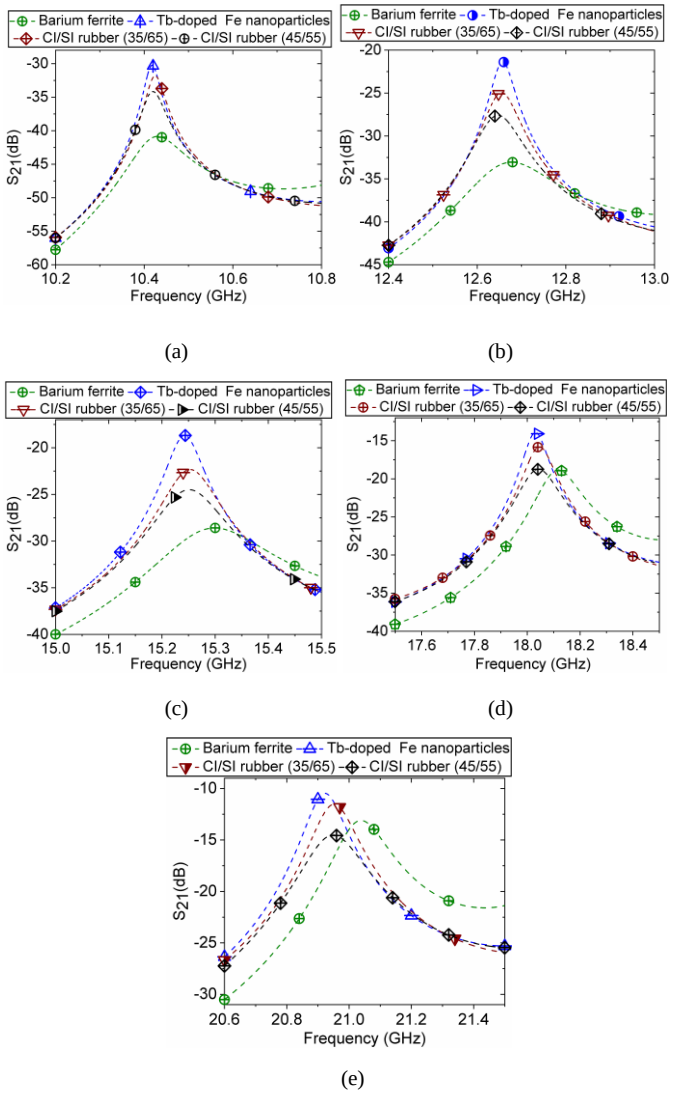

Fig. 9. Magnitude (dB) plot of measured transmission coefficient for each synthesized sample under test around the operating TE_{10p} mode for (a) p = 4, (b) p = 6, (c) p = 8, (d) p = 10, and (e) p = 12

From Fig.9, two interesting observation can be made, e.g., the shift in resonant frequency and quality factor are not uniform for a sample at each resonating TE_{10p} mode. This particular behavior of shift in frequency and quality factor was not considered in the conventional approach; however, the proposed scheme accounts for these changes and produce

quite accurate results. The second observation suggests that unlike the dielectric measurement, the perturbed frequency does not always less than the unperturbed frequency. The significance of the higher value of perturbed frequency than the unperturbed frequency is the diamagnetic behavior of the material under test, which can also be explained by (2). To estimate the value of the complex permeability of the synthesized sample, the recorded resonant frequency and quality factor corresponding to each mode of resonance are used in (3) and (7). For the sake of comparison and to show the clarity in the proposed approach, the calculated values of the complex permeability are plotted Fig. 10.

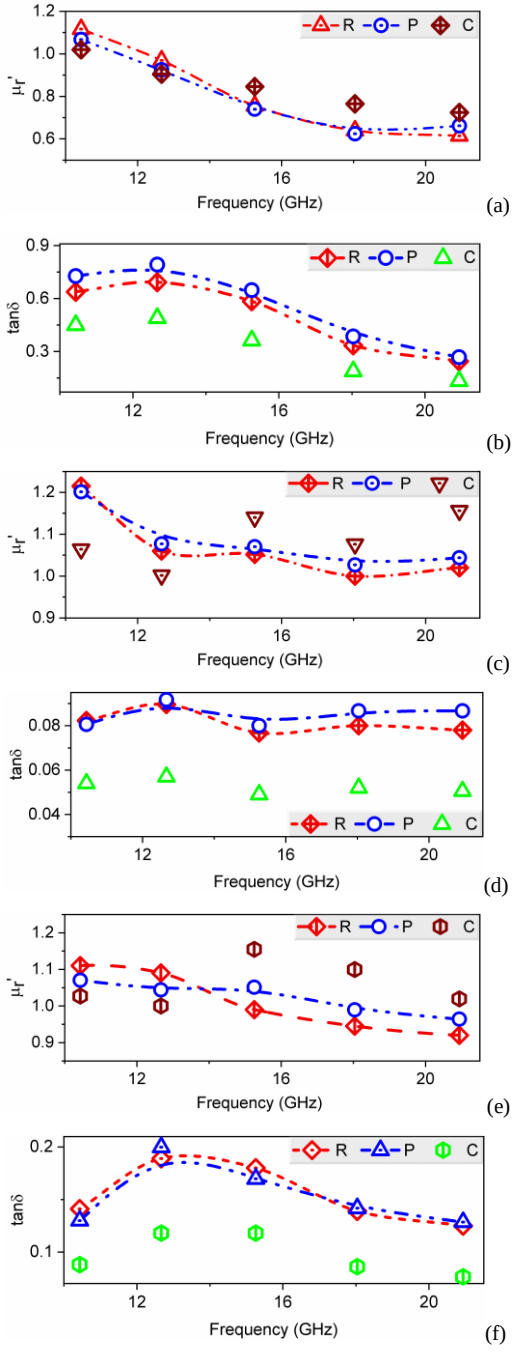

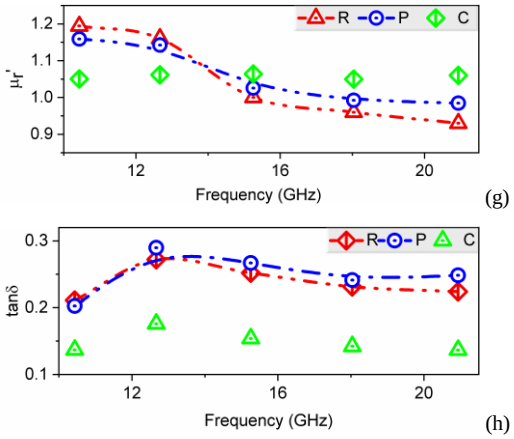

Fig. 10. Measured real permeability and magnetic loss tangent data of synthesized samples (a) and (b) barium ferrite, (c) and (d) Tb-doped Fe-nanoparticles, (e) and (f) CI/SI rubber (35/65), (g) and (h) CI/SI rubber (45/55) using the conventional (C) and the proposed (P) schemes. The reference (R) values of the synthesized dispersive sample are also given for reference.

The plot of reference values of complex permeability in Fig. 10 suggests that the synthesized samples are quite dispersive in nature. In this figure, except the Tb-doped ferrite (with iron nanoparticles), the rest three magnetic samples under test show the paramagnetic as well as diamagnetic behavior in the wideband of microwave frequency, where the paramagnetic characteristics are switched to diamagnetic with the increase in frequency. From Figs. 10(a), 10(c), 10(e) and 10(g), it may be noted that the values of real permeability obtained using the proposed multimodal SIW scheme and the continuous broadband plot obtained using the Debye model closely follow the dispersive reference values [23], [24], [27]-[30], while the results obtained using the conventional scheme does not follow the same. The differentiation in the measured results obtained using the two schemes, i.e., the conventional and the proposed schemes are profound in case of magnetic loss tangent data, which is mainly due to the use of the improvised quality factor in the proposed method as can be seen from Figs. 10(b), 10(d), 10(f) and 10(h). The error in the measurement of real permeability and magnetic loss tangent is calculated from the data, as represented in Fig. 10 and summarized in Table I. This table basically specifies the minim achieved accuracy using the proposed approach across all the modes. In this table, the percentage accuracy improvement corresponds to the real permeability (PAI_r), and magnetic loss tangent (PAI_δ) are introduced for quantifying the improvement in magnetic material characterization using the proposed method, which is calculated using the relation of absolute error as given in (8)

$$\mathrm{PAI}_r = \frac{\exists\mu'_{rP} - \exists\mu'_{rC}}{\mu'_{rAi}} \times 100\%$$
$$\mathrm{PAI}_\delta = \frac{\exists\tan\delta_{mP} - \exists\tan\delta_{mC}}{\tan\delta_{mA}} \times 100\% \quad (9)$$

where suffixes P and C represent the measured results calculated using the proposed and conventional techniques.

TABLE I: THE ACCURACY IN ESTIMATED PERMEABILITY AND THE PERCENTAGE ACCURACY IMPROVEMENT

Material Under Test	Accuracy of the proposed approach		Percentage accuracy improvement (PAI)	
	Real Permeability	Magnetic Loss Tangent	PAI_r	PAI_δ
Barium ferrite	92.27%	84.9%	17.52%	35.90%
Tb-doped Fe-nanoparticles	92.7%	89.10%	12.79%	34.29%
CI/SI rubber (35/65)	93.84%	92.13%	13.06%	36.96%
CI/SI rubber (45/55)	94.15%	89.07%	12.39%	35.04%

TABLE II: COMPARISON OF BROADBAND MICROWAVE CHARACTERIZATION TECHNIQUE USING SIW CAVITY

Methods► Attributes▼	[23]	[24]	[25]	This work
Frequency Range (GHz)	2-4	11-20	1-4	10-22
Number of Resonators	2	1	7	1
Permeability Estimation	X	X	✓	✓
Reference Sample	✓	X	✓	X
Specific to the Method	Multilayer Permittivity estimation of liquid	Single-layer, Permittivity estimation of small sample	Single-layer, Single-frequency measurement	Single-layer, Multimodal approach

A careful observation of columns 2, 4, and 3, 5 of Table I suggests that the real permeability and magnetic loss tangent data obtained using the proposed technique are more accurate than the conventional technique. The percentage accuracy improvement is calculated as the figure of merit, which quantifies the maximum improvement in the characterization of magnetic material using the proposed scheme over the conventional scheme. From columns 2 and 3 of Table I, it can be observed that the proposed technique typically provides more than 92% and 84% accuracy in the retrieval of real permeability and loss tangent data of sample under test, respectively, when tested in a wideband of microwave frequency 10 GHz -22 GHz. It can be noted from columns 4 and 5 of Table I that the PAI values of magnetic loss tangent real permeability data generated using modified formulation are 34% and 12 % better than that of the data obtained using the conventional approach. Moreover, to highlight the uniqueness and advantage of the work as compared to the state of art broadband microwave characterization technique using SIW cavity, a comparison of various schemes is provided in Table II. It can be observed from Table II that the proposed approach is capable of characterizing the complex permeability of a test specimen in the broadband microwave frequency exploiting the multimodal approach of single-layer single SIW cavity without the need of a reference sample.

IV. UNCERTAINTY ANALYSIS

This section mainly deals with the uncertainty analysis associated with the proposed magnetic characterization approach considering TE_{104} mode of SIW cavity. The uncertainty in measured complex permeability arising due to the effect of sample size, i.e., sample volume, sample misalignment and possible air-gap between sample and SIW cavity is numerically computed and sequentially explained. The uncertainty of the proposed scheme due to the errors in sample volume, sample misalignment, and air-gap are expressed in terms of percentage error and given in Figs. 11(a), (b), and (c), respectively corresponding to a typical test specimen A (1.2-j0.048) for 10 mm x 0.8 mm x 1 mm as its actual dimension. For a fair comparison, the uncertainty analysis is also performed for conventional method and plotted along with the proposed method. For an arbitrary sample, the sample size is uniformly varied in the limit of ±5% along y- and z- directions around the original dimension, and the results are plotted in Fig 11(a). From Fig 11(a), it can be observed that the proposed scheme produces the maximum error (±3.8%) less than ±5% for a ±5% change in sample volume, whereas the error in the extracted permeability using conventional approach gives nearly 10% error. For the sample misalignment, sample size is kept fixed while the sample misalignment up to 10% is considered along the positive x-direction, and accordingly, the percentage errors in complex permeability using (3) and (7) are estimated and plotted in Fig. 11(b). Since the sample misalignment would be an even function of x=0 plane, the negative values of error can be easily guessed from the data points given in Fig. 11(b). From Fig. 11(b), it can be observed that the maximum error in complex permeability using proposed scheme (~3.7%) is lower than 5%, while conventional scheme provides nearly 10% error. Since the magnetic field intensity is higher in the sample edges along the x- and y-directions as compared to z-direction, these two directions are chosen for the air-gap analysis. The air-gap is varied up to 10%, and accordingly the percentage error in the measurement of complex permeability using (3) and (7) is estimated. The plot of the percentage error in complex permeability due to the presence of finite air gap along the positive x- and y-directions for both the schemes is shown in Fig. 11(c). As the presence of air gap would be an even function of x=0 and y=0 plane, the negative values of error can be easily guessed from the data points given in Fig. 11(c). From this figure, it can be observed that the proposed approach may produce a maximum error (~3.5%) less than 5% whereas error in the extracted permeability using conventional approach is typically about 10% for a 10% air gap. Therefore, it can be concluded from Fig. 11 that the proposed scheme provides a better result than the conventional scheme even in the worst cases of the uncertainties in sample preparation and measurement.

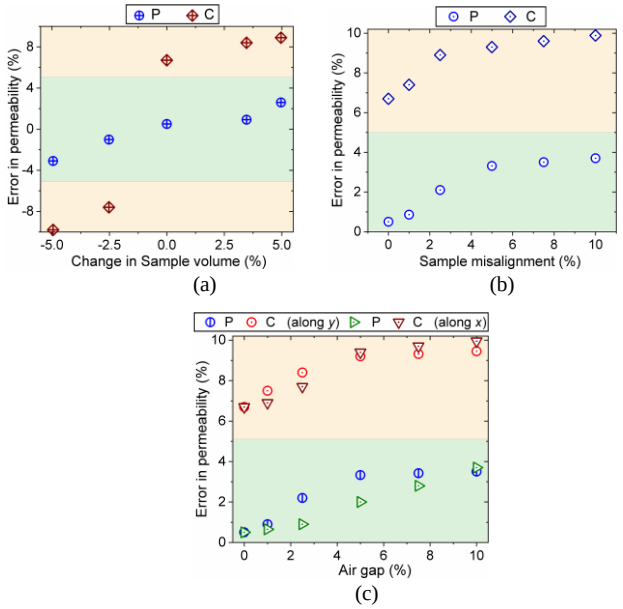

Fig. 11. Uncertainty analysis due to the (a) sample volume, (b) sample misalignment, (c) presence of finite air gap between the sample and SIW cavity.

As shown in Table I, in pragmatic conditions there might be simultaneous uncertainty in more than one input parameter, i.e., sample volume, and sample misalignment. In this situation maximum error in the extracted parameters might be increased ~ 8 % due to the presence of cumulative errors of individual parameters. Hence, the minimum achievable accuracy of the proposed method decided by the cumulative uncertainties in more than one input parameters which can be noticed from the Table I. In this table minimum realizable error in present scenario is ~92% which nearly comply with a typical cumulative error (~ 8 %) generated due the uncertainty in more than one input parameters in Fig. 11.

V. Conclusion

A unique technique has been developed for the broadband characterization of magnetic materials using the multimode operation of the SIW cavity at the microwave frequency. A new formulation has been developed from the first principle, which is tested and verified using several standards and synthesized magnetic materials. The developed scheme exclusively relaxes both the significant limitations of the conventional SIW cavity constraints as well as the inherent constraints of the conventional cavity perturbation approach. The modified coupling proposed for the SIW cavity improves the quality factor as compared with the conventional SIW cavity. The proposed formulation eradicates the need for additional standard magnetic samples generally used for calibration, and also relieves the need for multiple cavities for characterizing the magnetic sample over the broad frequency range. The viability of the scheme is numerically tested with a detailed uncertainty analysis and found to be better than the conventional scheme. The proposed planar technique has been found to be quite useful for characterization of a magnetic sample with high precision, which can be very useful for microwave material processing industry.

References

[1] K. T. Mathew, "Perturbation theory," in *Encyclopedia of RF and Microwave Engineering*, vol. 4. New York, NY, USA: WileyInterscience, 2005, pp. 3725–3735.

[2] R. A. Waldron, "Perturbation theory of resonant cavities," *Proc. Inst. Elect. Eng.*, vol. 107, pp. 272–274, Sep. 1960.

[3] R. F. Harrington, *Time-Harmonic Electromagnetic Fields*. New York, NY, USA: Wiley-Interscience, 2001, pp. 317–349.

[4] J. Krupka, "Frequency domain complex permittivity measurements atmicrowave frequencies," *Meas. Sci. Technol.*, vol. 17, pp. R55–R70, Sep. 2005.

[5] K. P. Thakur and W. S. Holmes, "An inverse technique to evaluate permittivity of material in a cavity," *IEEE Trans. Microw. Theory Techn.*, vol. 49, no. 6, pp. 1129–1132, Jun. 2001.

[6] L. Chen, C. K. Ong, and B. T. G. Tan, "Amendment of cavity perturbation method for permittivity measurement of extremely low-loss dielectrics," *IEEE Trans. Instrum. Meas.*, vol. 48, no. 6, pp. 1031–1037, Dec. 1999.

[7] A. Verma and D. C. Dube, "Measurement of dielectric parameter of small samples at X-band frequencies by cavity perturbation technique," *IEEE Trans. Instrum. Meas.*, vol. 54, no. 5, pp. 2120–2123, Oct. 2005

[8] A. K. Jha and M. J. Akhtar, "A generalized rectangular cavity approach for determination of complex permittivity of materials," *IEEE Trans.Instrum. Meas.*, vol. 63, no. 11, pp. 2632–2641, Nov. 2014.

[9] U. Raveendranath and K. T. Mathew, "New cavity perturbation technique for measuring complex permeability of ferrite materials," *Microw. Opt.Technol. Lett.*, vol. 18, no. 4, pp. 241–243, Jul. 1998.

[10] R. B. Yang, C. Y. Tsay, D. S. Hung, W. F. Liang, Y. D. Yao, and C. K. Lin, "Complex permittivity and permeability of iron-based composite absorbers measured by cavity perturbation method in X-band frequency range," *J. Appl. Phys.*, vol. 105, no. 7, pp. 07A528-1–07A528-3, 2009.

[11] R. B. Yang, W. F. Liang, W. S. Lin, H. M. Lin, C. Y. Tsay, and C. K. Lin, "Microwave absorbing properties of iron nanowire at X-band frequencies," *J. Appl. Phys.*, vol. 109, no. 7, p. 07B527, 2011.

[12] L. F. Chen, C. K. Ong, C. P. Neo, V. V. Varadan, and V. K. Varadan, *Microwave Electronics: Measurement and Materials Characterization*.London, U.K.: Wiley, 2004.

[13] A. K. Jha and M. J. Akhtar, "An improved rectangular cavity approach for measurement of complex permeability of materials," *IEEE Trans.Instrum. Meas.*, vol. 64, no. 4, pp. 995–1003, Apr. 2015.

[14] A. K. Jha and M. J. Akhtar, "Improved Resonator Method for Microwave Testing of Magnetic Composite Sheets," *IEEE Trans. Magn.*, vol. 51, no. 9, pp. 1-9, Sept. 2015.

[15] A. K. Jha, N. K. Tiwari, and M. J. Akhtar, "Novel microwave resonant technique for accurate testing of magnetic materials," *IEEE Trans. Microw. Theory Techn.*, vol. 67, no. 1, pp. 239-248, Jan. 2019.

[16] L. Silvestri, E. Massoni, C. Tomassoni, A. Coves, M. Bozzi, and L. Perregrini, "Substrate integrated waveguide filters based on a dielectric layer with periodic perforations," *IEEE Trans. Microw. Theory Techn.*, vol. 65, no. 8, pp. 2687–2697, Aug. 2017.

[17] C. Tomassoni, L. Silvestri, A. Ghiotto, M. Bozzi, and L. Perregrini, "Substrate-integrated waveguide filters based on dual-mode air-filled resonant cavities," *IEEE Trans. Microw. Theory Techn.*, vol. 66, no. 2, pp. 726–736, Feb. 2018.

[18] R. A. Alahnomi, Z. Zakaria, E. Ruslan, S. R. Ab Rashid, and A. A. Mohd Bahar, "High-Q sensor based on symmetrical split ring resonator with spurlines for solids material detection," *IEEE Sensors J.*, vol. 17, no. 9, pp. 2766-2775, May, 2017.

[19] M. A. H. Ansari, A. K. Jha and M. J. Akhtar, "Design and application of the CSRR-based planar sensor for noninvasive measurement of complex permittivity," *IEEE Sensors J.*, vol. 15, no. 12, pp. 7181-7189, Dec. 2015.

[20] K. Saeed, R. D. Pollard, and I. C. Hunter, "Substrate integrated waveguide cavity resonators for complex permittivity characterization of materials," *IEEE Trans. Microw. Theory Techn.*, vol. 56, no. 10, pp. 2340–2347, Oct. 2008.

[21] H. Lobato-Morales, A. Corona-Chávez, D. V. B. Murthy, and J. L. Olvera-Cervantes, "Complex permittivity measurements using cavity perturbation technique with substrate integrated waveguide cavities," *Rev. Sci. Instrum.*, vol. 81, no. 6, p. 064704, Jun. 2010.

[22] H. Lobato-Morales, D. V. B. Murthy, A. Corona-Chavez, J. L. Olvera-Cervantes, J. Martinez-Brito, and L. G. Guerrero-Ojeda, "Permittivity measurements at microwave frequencies using epsilon near-zero (ENZ)

tunnel structure," *IEEE Trans. Microw. Theory Techn.*, vol. 59, no. 7, pp. 1863–1868, Jul. 2011.
[23] A. K. Jha and M. J. Akhtar, "Design of multilayered epsilon-near-zero microwave planar sensor for testing of dispersive materials," *IEEE Trans. Microw. Theory Techn.*, vol. 63, no. 8, pp. 2418–2426, Aug. 2015.
[24] N. K. Tiwari, A. K. Jha, S. P. Singh, Z. Akhter, P. K. Varshney, and M. J. Akhtar, "Generalized multimode SIW cavity-based sensor for retrieval of complex permittivity of materials," *IEEE Trans. Microw. Theory Techn.*, vol. 66, no. 6, pp. 3063-3072, June 2018.
[25] K. Han *et al.*, "RF characterization of magnetodielectric material using cavity perturbation technique," *IEEE Trans. Compon., Packag., Manuf. Technol.*, vol. 5, no. 12, pp. 1850–1859, Dec. 2015.
[26] D. M. Pozar, *Microwave* Engineering, 3rd ed. New York, NY, USA: Wiley, 1989.
[27] Snoek, J. L. "Dispersion and absorption in magnetic ferrites at frequencies above one Mc/s."*Physica* 14.4 (1948): 207-217.
[28] B. Feng T. Qiu C. Y. Shen "Absorbing properties and structural design of microwave absorbers based on carbonyl iron and barium ferrite" J. Magn. Magn. Mater. vol. 318 pp. 8-13, 2007.
[29] Z. Han et al., "Permittivity and permeability of Zn(Fe)/ZnO nanocapsules and their microwave absorption in the 2–18 GHz range," J. Appl. Phys., vol. 115, no. 17, 2014, (17A527).
[30] A. M. Gama and M. C. Rezende, "Complex permeability and permittivity variation of carbonyl iron rubber in the frequency range of 2 to 18 GHz, *J. Aerosp. Technol. Manage.*, vol. 2, no. 1, pp. 59–62, 2011.

Nilesh K. Tiwari (Student Member, IEEE) is currently pursuing the Ph.D. degree with the Electrical Engineering Department, IIT Kanpur, Kanpur, India.

Abhishek K. Jha (Member, IEEE) is with the Department of Microwave and Antenna Engineering, Electronics, Telecommunications and Informatics (ETI) Faculty, Gda´nsk University of Technology, Gda´nsk, Poland.

S. P. Singh (Student Member, IEEE) is currently pursuing the Ph.D. degree with the Electrical Engineering Department, IIT Kanpur, Kanpur, India.

M. Jaleel Akhtar (Senior Member, IEEE) is currently a Professor with the Electrical Engineering Department, IIT Kanpur, Kanpur, India